



Contents lists available at ScienceDirect

Geoderma

journal homepage: www.elsevier.com/locate/geoderma

Toward process-based modeling of geochemical soil formation across diverse landforms: A new mathematical framework

Kyungsoo Yoo^{a,*}, Simon Marius Mudd^b

^a University of Delaware, Plant and Soil Sciences Department, Department of Geological Sciences, Newark, DE, USA

^b School of GeoSciences, University of Edinburgh, UK

ARTICLE INFO

Article history:

Received 15 September 2007

Received in revised form 15 April 2008

Accepted 29 May 2008

Available online xxx

Keywords:

Soil formation

Land forms

Modeling

Physical weathering

Chemical weathering

ABSTRACT

We present a mathematical model that integrates geochemical and geomorphic processes responsible for soils' elemental and mineralogical evolution on diverse landforms: eroding to depositional to level grounds. This new model combines a hillslope sediment mass balance and a soil geochemical mass balance. We model soils as the sum of a physically disturbed zone (PDZ) and the underlying physically undisturbed but chemically altered zone (CAZ). The model considers processes including the production of PDZ, weathering front propagation, mineral-specific dissolution, colloidal translocation, and colluvial transport. Thus this study serves to (1) review preexisting models of pedogenic processes and to (2) offer a framework to integrate the geochemical and geomorphic processes active in soils. We further discuss the implications of our model in (1) scaling chemical weathering reactions from mineral grains to pedons to soil catenas, (2) understanding the emergence of geochemical soil catenas, and (3) coupling physical and chemical weathering processes.

© 2008 Published by Elsevier B.V.

1. Introduction

Elemental or mineralogical compositions of soils evolve due to complex feedbacks among geochemical and geomorphic processes within and at the boundaries of the soil layer. Geochemical processes involve dissolution, leaching, precipitation, and colloidal translocation, whereas geomorphic processes include the conversion of parent material to soil materials and the colluvial transport of the soil materials. Mathematical modeling that functionally relates these processes to the evolution of elemental and mineralogical compositions of soil from unweathered bedrock to the soil surface could bear significant insight into advancing our knowledge of soil formation and its interaction with the evolution of landscape morphology. Kirkby (1977, 1985) presented models of soil profile development within the context of eroding hillslopes, but in the time since this pioneering work relatively few attempts have been made to couple geochemical soil formation and geomorphic processes despite a number of significant advances in both hillslope sediment transport and geochemical mass balance techniques.

Whereas some pedogenic models have focused on the energy fluxes through soil systems [e.g., Rasmussen and Tabor, 2007], most conceptual models of soil formation involve processes responsible for mass additions, removals, translocation, and transformation (Simonson, 1959). Though qualitative in nature, the concept still provides powerful insights into linking observed soil properties and processes

(Schaeztl and Anderson, 2005). The geochemical mass balance approach (Marshall and Haseman, 1942; April et al., 1986; Brimhall and Dietrich, 1987), which embodies the concept of Simonson (1959), has proven to be a powerful method to quantify mass losses, gains, and translocation during the soil formation.

In addition to geochemical alteration within a soil, mass inputs and outputs through the boundaries of the soil directly affect the geochemical composition of the soil profile. Those mass fluxes are responsible for lowering the land surface or the soil-bedrock interface. In the time since its introduction by Culling (1963), the mass balance approach to hillslope sediment (i.e., colluvial soil) transport has matured into a widely used tool for geomorphic analysis (e.g., Dietrich et al., 1995). Such mathematical analyses are increasingly combined with denudation rates determined with cosmogenic radionuclides (e.g., Heimsath et al., 1997; Bierman and Nichols, 2004) and/or topographic surveys (Heimsath et al., 1999). These advances in hillslope geomorphology, together with the successes of the geochemical mass balance, lay the foundations for quantitatively integrating geomorphic and geochemical processes in modeling of soil formation.

Recently the quantitative separation of the mass losses via physical vs. chemical weathering from soils has been made at catchment scales (Riebe et al., 2003a,b, 2004). In addition, the spatial variation of soil chemical weathering rates and their contribution to denudation within hillslope transects is beginning to be quantified (Nezat et al., 2004; Green et al., 2006; Yoo et al., 2007) and considered in modeling the geomorphic evolution of hillslopes (Mudd and Furbish, 2004). These advances provide opportunities to pursue the co-evolution of soil geochemistry and hillslope morphology through a unifying

Q1

* Corresponding author.

E-mail addresses: kyoo@udel.edu (K. Yoo), simon.m.mudd@ed.ac.uk (S.M. Mudd).

mathematical model (e.g., Minasny and McBratney, 1999, 2001; Yoo et al., 2005b, 2006; Minasny and McBratney, 2006; Yoo et al., 2007), but a comprehensive and quantitative framework is lacking. Filling this gap is the purpose of this study.

2. Background and issues

The geochemical mass balance (Marshall and Haseman, 1942; Brimhall and Dietrich, 1987) has been applied to soils formed from underlying parent material (an exception being cases where aeolian inputs are considered, e.g., Brimhall et al., 1988). The total mass loss, δ [$M L^{-2}$], during soil formation is described as

$$\delta = \left(\frac{C_{iw}}{C_{ir}} - 1 \right) \rho_w h_w, \quad (1a)$$

and the mass loss rate by chemical weathering S [$M L^{-2} T^{-1}$] is

$$S = \frac{\partial \delta}{\partial t}, \quad (1b)$$

where C is mass concentration [$M M^{-3}$], ρ_w is soil bulk density [$M L^{-3}$], h_w is soil thickness [L], t is soil age which is equivalent of the time since the cessation of erosion or deposition [T], the subscript i represents weathering resistant index elements or minerals, and the subscripts w and r represent soil and parent material, respectively. While this approach has been successful in studying soil chronosequences (Amundson, 2004), it is not applicable to eroding or depositional landscapes: the soil age cannot be defined because erosion and deposition continuously rejuvenate the soils (Almond et al., 2007; Yoo et al., 2007; Yoo and Mudd, 2008). Additionally, the parent material for eroding or depositional soil is poorly defined due to sediment input from upslope (Mudd and Furbish, 2006; Yoo et al., 2007).

In contrast, geomorphologists have described the soil-mantled landscapes by including the physical conversion of bedrock to colluvial soil (referred to as colluvial soil production) and the physical removal of that soil but without considering the mass fluxes due to chemical weathering (Dietrich et al., 1995; Heimsath et al., 1997):

$$\frac{\partial(\rho_w h_w)}{\partial t} = \rho_r p - \nabla \cdot (\rho_w \vec{Q}_w), \quad (2)$$

in which h_w is the thickness of colluvial soil [L], p is the production rate of the colluvial soil [$L T^{-1}$], and Q_w is the volume of colluvial flux crossing across a unit length of a contour line (referred to as sediment flux in geomorphic literature) [$L^2 T^{-1}$]. The divergence of mass sediment flux is equal to soil erosion rate which has the dimension of mass per area per time.

In summary, colluvial soil production and colluvial transport have not been considered in the geochemical evolution of soils (Eq. (1)) and chemical weathering has been neglected in understanding the geomorphology of soil covered hillslopes (Eq. (2)). The division between the two approaches was first addressed by Riebe et al. (2001, 2003a,b, 2004). They separately quantified long term rates of soil chemical weathering and physical soil erosion at catchment scales under two assumptions: 1) the catchment denudation rate is in equilibrium with the rate of soil production and 2) the catchment soils' elemental composition does not change over time because of the continuous removal of the soils by physical erosion. Riebe et al. (2001, 2003a,b, 2004) found that the mass loss rate via chemical weathering from colluvial soil within a catchment may be calculated by quantifying the enrichment of weathering resistant soil components and soil production rates:

$$S = \left(1 - \frac{C_{ir}}{C_{iw}} \right) \rho_r p. \quad (3)$$

This model, however, has limited utility in understanding soils' geochemical catena because of the steady state assumption and its nature of averaging out the topographic variation of soils.

More comprehensive models for determining the soil chemical weathering rate as a function of hillslope position were recently developed (Mudd and Furbish, 2006; Yoo et al., 2007). If one assumes a soil's mass and chemical composition are in steady state, the chemical weathering rate can be described as a function of the topographic variation of colluvial soils' elemental composition, the production rate of colluvial soil, and the colluvial flux (Mudd and Furbish, 2006; Yoo et al., 2007):

$$S = \left(1 - \frac{C_{ir}}{C_{iw}} \right) \rho_r p + \frac{\nabla C_{iw}}{C_{iw}} \rho_w \cdot \vec{Q}_w. \quad (4) \quad 141$$

For the detailed derivation of Eq. (4), see Yoo et al. (2007). 139

This most recent model (Eq. (4)) (Mudd and Furbish, 2006; Yoo et al., 2007) still lacks several essential features required for integrating geomorphic processes and soils' geochemical evolution. The model defines soils in a way that differs from most pedogenesis studies. In pedological studies, a soil includes colluvial soil as a subset of the entire soil profile without explicitly identifying physically disturbed colluvial soil from physically undisturbed material. In contrast, the application of models described in Eqs. (2), (3), and (4) is limited to the colluvial component of a soil. 150

Additionally, steady state assumptions need to be relaxed. Due to the continuous rejuvenation of the soil via erosion and soil production, many geomorphic studies have assumed that the soil layer on eroding hillslopes is in steady state (e.g., Heimsath et al., 1999). Such mass replacements do not occur for depositional soils or soils on level grounds. In addition, a number of studies have found evidence for transient behavior both in terms of geochemistry (e.g., Birkeland and Berry, 1991) and soil thickness (e.g., Birkeland and Berry, 1991; Roering et al., 2004; Roering and Gerber, 2005) on eroding hillslopes. Indeed, hillslopes' response to changes in climate and tectonics occurs at the timescales that are longer than the period of recent glacial and interglacial cycles (Fernades and Dietrich, 1997; Roering et al., 2001; Mudd and Furbish, 2007). 163

3. Model development

3.1. Defining a soil system

We begin with a soil of thickness h and unit area (1 m^2) at the soil surface; this volume is often the smallest observable unit of soil called a pedon (Fig. 1). The arbitrary nature of defining the vertical extent of soils (Jenny, 1941) has resulted in numerous terms for a certain vertical portion of the materials mantling unweathered geological materials (Tandarich et al., 2002). One immediate problem we face in this study is to set the boundary between colluvial soil and in-situ soil. Despite the elaborate schemes of determining soil horizons based on various morphologic features including color, texture and structure (Buol et al., 1997) and the acknowledgement of physically mixed soil zone (Johnson, 1990), current soil surveys (Soil Survey Division Staff, 1993) do not explicitly factor the physical soil disturbance in dividing master horizons. 178

We consider a soil as the sum of two distinct layers: a physically disturbed soil zone (hereafter PDZ) and a physically undisturbed but chemically altered soil zone (hereafter CAZ). In the PDZ, materials are physically perturbed by animal burrowing, the growth and decay of plant roots, tree falls, shrinking and swelling of 2:1 clay minerals, etc (e.g., Carson and Kirkby, 1972; Hole, 1961, 1981; Gabet et al., 2003). When organisms cause the physical perturbation, the PDZ is equivalent to the biomantle (Johnson, 1990). On hillslopes, the PDZ is synonymous with colluvial soil, which was the object of the mass balance described in Eqs. (2), (3) and (4). The PDZ includes at least A horizons. In the grass covered hillslopes in Coastal California where the colluvial soil production function was first empirically quantified (Heimsath et al., 1997), the colluvial soil is a well mixed dark A horizon 191

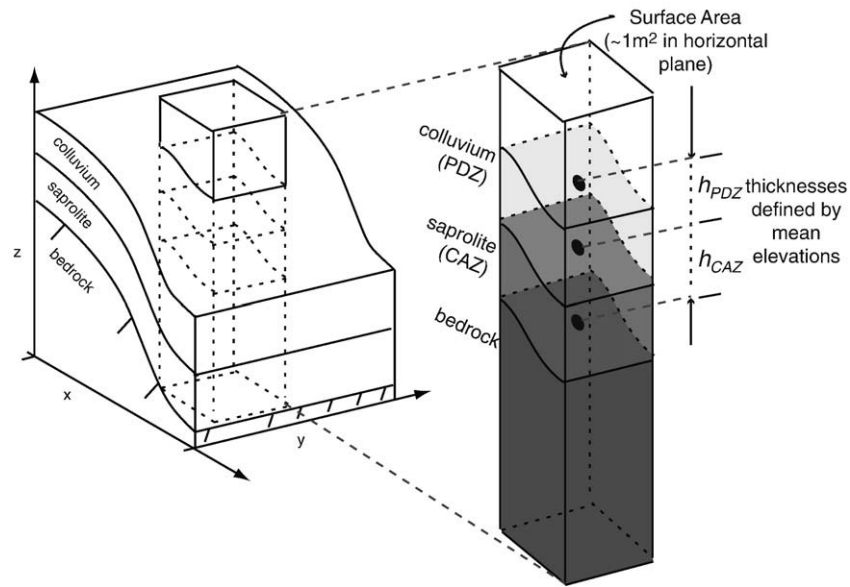


Fig. 1. Schematic of the modeled soil system at the pedon scale.

192 overlying a clay rich saprolite or Bt horizon (Monaghan et al., 1992;
 193 McKean et al., 1993; Heimsath et al., 1997; Yoo et al., 2005a, 2006).
 194 In other circumstances, the PDZ may include the B horizon in its entirety
 195 or a portion thereof. Some B horizon materials may continuously mix
 196 with the overlying A horizon without retaining a low value of the
 197 Munsell color system (Munsell Color, 2000) because of the lack of
 198 organic matter. Indeed, in the semi-arid highlands in Southeast
 199 Australia, the bioturbated colluvial soil includes Bw horizons
 200 (Heimsath et al., 2000; Heimsath et al., 2001a; Yoo et al., 2007).

201 In the PDZ, continuous physical perturbations lead to gross lateral
 202 mass flux (q_{PDZ}) where this flux is defined as the volume of materials
 203 crossing a unit contour line per unit time [$L^2 T^{-1}$]. Mathematically, the
 204 PDZ is a layer in which the gross lateral mass flux has non-zero values.
 205 Note that the gross flux is a vector; it has both direction and quantity:

$$206 \vec{q}_{PDZ} \neq 0. \quad (5)$$

207
 208
 209 Chemical alteration of minerals, in general, extends beyond the
 210 PDZ; virtually all mature soils exhibit a CAZ underneath the PDZ.
 211 Water, dissolved or colloidal organic acids, oxidizing ions, and
 212 microorganisms travel through pores, and the diurnal to seasonal
 213 cycles of soil moisture and temperature temper out with increasing
 214 soil depth. One notable example of the CAZ is saprolite of which the
 215 original definition is "thoroughly decomposed, earthy, but *untrans-*
 216 *ported* rock" (Becker, 1895; Tandarich et al., 2002). The CAZ, as
 217 noted earlier, may include a portion or all of the B horizons. Physical
 218 disturbance in the B horizon is, however, poorly understood. Even at
 219 depths where soil perturbing animals cannot reach, prolonged
 220 chemical weathering may result in the volumetric collapse of the
 221 soil matrix (Merritts et al., 1992). In this study, we do not consider such
 222 chemical weathering driven collapse as a part of physical soil
 223 perturbation. In soils with B horizons such as duripan, fragipan and
 224 placic horizon, bioturbation could be further limited to the overlying
 225 horizons, as dense clay layers prevent the access of soil bioturbators.
 226 Stone lines, which are interpreted as materials too big or heavy for
 227 bioturbation, virtually always occur at the interface between A and B
 228 horizons (Johnson, 1994). Thus, in many cases (but not in every case)
 229 the boundary between the PDZ and CAZ occurs at the boundary
 230 between the A and B horizons.

231 Mathematically, the CAZ is defined by the absence of gross material
 232 movements. The CAZ may develop a diffuse boundary with the
 underlying fresh parent material and thus this boundary should be

233 considered an idealization for the mathematical treatment. We define
 234 the lower boundary as the deepest depth where detectable mass loss
 235 via dissolution and leaching is found for at least one element or a
 mineral species (subscript j):

$$236 \vec{q}_{CAZ} = 0, \quad (6a) \quad 238$$

237 and

$$239 \delta_{j,CAZ} = \left(C_{j,r} \frac{C_{i,CAZ}}{C_{i,r}} - C_{j,CAZ} \right) \rho_{CAZ} h_{CAZ} \neq 0. \quad (6b) \quad 241$$

242 Although volumetric change is not considered in dividing a soil
 243 profile into the two layers, in general, bioturbation tends to increase
 the volume of a given soil material.

244 We acknowledge that the models presented in this study have the
 245 risk of oversimplifying soil profiles. Biological and physical soil
 246 perturbation and chemical weathering, however, are universal and
 247 extend to different maximum depths. Additionally, the model
 248 development below illustrates that even for this simplified soil profile,
 249 the basic processes contributing to geochemical evolution of soils
 250 have not been well identified and measured. Though promising
 251 multilayered models of soils have been constructed (e.g., Salvarodr-
 252 Blanes et al., 2007), these models have not included lateral sediment
 253 fluxes that occur on eroding hillslopes, nor have these models ex-
 254 plicitly incorporated the geochemical mass balance. As our computa-
 255 tional power grows and empirical data on major mass fluxes as a
 256 function of soil depth accumulates, our models can be also extended to
 include a number of soil layers.

3.2. Governing mass balances 258

3.2.1. Mass balance of the PDZ 259

260 Among many properties characterizing the PDZ, we track its bulk
 261 mass and the amounts of weathering susceptible soil elements or
 262 mineral species and weathering resistant soil components as a
 263 function of time. Typical insoluble elements include Zr, Ti, and Nb,
 264 which commonly reside in chemically resistant oxide minerals such as
 265 zircon and rutile (e.g., Nb in Kurtz et al., 2000, Zr in Brimhall et al.,
 1988). The mineral quartz has been also used as an index soil
 266 component (White et al., 1996).

267 A PDZ mass budget is determined by the production of the PDZ
 268 from the CAZ or fresh parent material, aeolian deposition, colluvial
 269

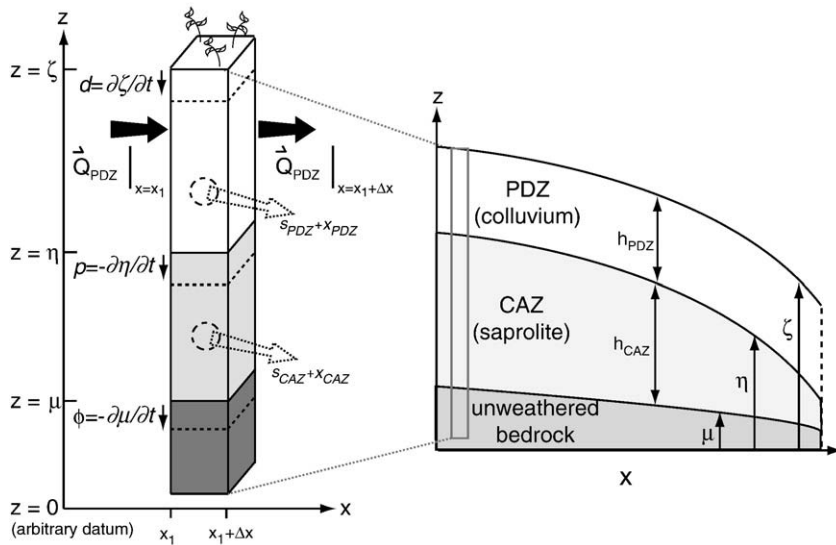


Fig. 2. Schematic of the modeled soil system. Note that d is defined as positive up, whereas p and ϕ are defined as positive down. In the schematic we show Q_{PDZ} , S_{PDZ} , x_{PDZ} , S_{CAZ} , and x_{CAZ} as local values (no overbars), whereas in the model mass balances are calculated using depth-averaged values.

fluxes, chemical weathering, and clay translocation. The chemical weathering rate is defined as the rate of net mass loss or gain via dissolution, precipitation, and leaching in the PDZ. The mass balance of insoluble soil components, however, is not affected by chemical weathering. Translocation terms represent the eluviation or illuviation of clay sized minerals.

The PDZ has an upper boundary at the elevation (z) of ζ and a lower boundary of η such that the thickness of the PDZ is $h_{PDZ} = \zeta - \eta$ (Fig. 2). The reference elevation (z) to which the vertical boundary conditions of a PDZ are measured could be defined differently depending on research questions. The mass balances of the bulk materials, weathering susceptible soil components with subscript j (e.g., the element Ca or the mineral plagioclase), and weathering resistant soil components with subscript i (e.g., element Ti or mineral zircon) in the PDZ are respectively:

$$\frac{\partial(\bar{\rho}_{PDZ}h_{PDZ})}{\partial t} = \rho_{\eta}p + \rho_{\zeta}d - \nabla \cdot (\bar{\rho}_{PDZ}\bar{Q}_{PDZ}) - h_{PDZ}(\bar{s}_{PDZ} + \bar{x}_{PDZ}), \quad (7a)$$

$$\frac{\partial(\bar{\rho}_{PDZ}\bar{C}_{j,PDZ}h_{PDZ})}{\partial t} = \rho_{\eta}C_{j,\eta}p + \rho_{\zeta}C_{j,\zeta}d - \nabla \cdot (\bar{\rho}_{PDZ}\bar{C}_{j,PDZ}\bar{Q}_{PDZ}) - h_{PDZ}(\bar{s}_{j,PDZ} + \bar{x}_{j,PDZ}), \quad (7b)$$

and

$$\frac{\partial(\bar{\rho}_{PDZ}\bar{C}_{i,PDZ}h_{PDZ})}{\partial t} = \rho_{\eta}C_{i,\eta}p + \rho_{\zeta}C_{i,\zeta}d - \nabla \cdot (\bar{\rho}_{PDZ}\bar{C}_{i,PDZ}\bar{Q}_{PDZ}) - h_{PDZ}\bar{x}_{i,PDZ}, \quad (7c)$$

where d is a deposition (if positive, e.g., aeolian deposition) or erosion (if negative, e.g., overland flow) rate at the surface of the PDZ [$L T^{-1}$], s is the rate that soil mass is lost or gained via chemical weathering per unit soil volume [$M L^{-3} T^{-1}$], x is the rate that soil mass is gained or lost due to clay translocation per unit soil volume [$M L^{-3} T^{-1}$] (Fig. 2). Terms with overbars are depth-averaged values such that, for example:

$$\bar{C}_{j,PDZ} = \frac{1}{h_{PDZ}} \int_{\eta}^{\zeta} C_{j,PDZ} dz. \quad (8)$$

Subsequently, the weathering rate from the PDZ (S_{PDZ} , with the dimension of $M L^{-2} T^{-1}$) is $S_{PDZ} = h_{PDZ} \bar{s}_{PDZ}$. Where the PDZ directly

overlies fresh parent material, which is often the case of young soils, subscript η should be replaced by r which represents fresh parent material. Production of the PDZ is defined as positive. If mass is lost due to either chemical weathering or translocation the terms s and x are positive, respectively.

The functional relationship between the rates of the processes shaping the PDZ can be stated by combining Eqs (7a)–(c):

$$\begin{aligned} \frac{\partial \bar{C}_{j,PDZ}}{\partial t} = & \frac{\rho_{\eta}p}{\bar{\rho}_{PDZ}h_{PDZ}} (C_{j,\eta} - \bar{C}_{j,PDZ}) + \frac{\rho_{\zeta}d}{\bar{\rho}_{PDZ}h_{PDZ}} (C_{j,\zeta} - \bar{C}_{j,PDZ}) \\ & - \frac{\bar{Q}_{PDZ}}{h_{PDZ}} \nabla \bar{C}_{j,PDZ} + \frac{(\bar{C}_{j,PDZ}\bar{s}_{PDZ} - \bar{s}_{j,PDZ})}{\bar{\rho}_{PDZ}} \\ & + \frac{(\bar{C}_{j,PDZ}\bar{x}_{PDZ} - \bar{x}_{j,PDZ})}{\bar{\rho}_{PDZ}} \end{aligned} \quad (9a) \quad 309$$

and

$$\begin{aligned} \frac{\partial \bar{C}_{i,PDZ}}{\partial t} = & \frac{\rho_{\eta}p}{\bar{\rho}_{PDZ}h_{PDZ}} (C_{i,\eta} - \bar{C}_{i,PDZ}) + \frac{\rho_{\zeta}d}{\bar{\rho}_{PDZ}h_{PDZ}} (C_{i,\zeta} - \bar{C}_{i,PDZ}) \\ & - \frac{\bar{Q}_{PDZ}}{h_{PDZ}} \nabla \bar{C}_{i,PDZ} + \frac{\bar{C}_{j,PDZ}\bar{s}_{PDZ}}{\bar{\rho}_{PDZ}} + \frac{(\bar{C}_{j,PDZ}\bar{x}_{PDZ} - \bar{x}_{j,PDZ})}{\bar{\rho}_{PDZ}}. \end{aligned} \quad (9b) \quad 311$$

The first two terms to the right of the equality in Eqs. (9a) and (9b) are the enrichment or depletion of the soil component i or j due to the production of the PDZ and aeolian deposition (or runoff erosion) respectively. The third term is the enrichment or depletion due to colluvial transport. The fourth term is the enrichment or depletion of a chemically soluble species due to chemical weathering, whereas the fifth term is the enrichment or depletion of the soil component i or j due to clay translocation.

3.2.2. Mass balance of the CAZ

The PDZ is coupled to the CAZ through production of the PDZ. The lower boundary of the CAZ is at an elevation of $z = \mu$ such that the thickness of the CAZ is $h_{CAZ} = \eta - \mu$ (Fig. 2). The mass balances of the bulk materials, weathering susceptible element (mineral j), and weathering resistant element (mineral i) in the CAZ are:

$$\frac{\partial(\bar{\rho}_{CAZ}h_{CAZ})}{\partial t} = \rho_{\mu}\phi - \rho_{\eta}p - h_{CAZ}\bar{s}_{CAZ} - h_{CAZ}\bar{x}_{CAZ}, \quad (10a)$$

$$\frac{\partial (\bar{\rho}_{CAZ} \bar{C}_{j,CAZ} h_{CAZ})}{\partial t} = \rho_r C_{j,r} \phi - \rho_\eta C_{j,\eta} p - h_{CAZ} \bar{s}_{j,CAZ} - h_{CAZ} \bar{x}_{j,CAZ}, \quad (10b)$$

and

$$\frac{\partial (\bar{\rho}_{CAZ} \bar{C}_{i,CAZ} h_{CAZ})}{\partial t} = \rho_r C_{i,r} \phi - \rho_\eta C_{i,\eta} p - h_{CAZ} \bar{x}_{i,CAZ}, \quad (10c)$$

where the subscript r represents fresh parent material, and ϕ is the weathering front propagation rate at the boundary between the CAZ and fresh parent material [$L T^{-1}$]. The overbars again indicate a depth-averaged quantity within the CAZ, for example,

$$\bar{C}_{j,CAZ} = \frac{1}{h_{CAZ}} \int_0^h C_{j,CAZ} dz. \quad (11)$$

As we have done for the PDZ (9a)-(b) we solve Eqs. (10a)-(c) to arrive at the changes in elemental or mineralogical compositions of the CAZ over time as a function of physical and chemical processes within and at the boundaries of the CAZ.

$$\frac{\partial \bar{C}_{j,CAZ}}{\partial t} = \frac{\rho_r \phi}{\bar{\rho}_{CAZ} h_{CAZ}} (C_{j,r} - \bar{C}_{j,CAZ}) - \frac{\rho_\eta p}{\bar{\rho}_{CAZ} h_{CAZ}} (C_{j,\eta} - \bar{C}_{j,CAZ}) + \frac{(\bar{C}_{j,CAZ} \bar{s}_{CAZ} - \bar{s}_{j,CAZ})}{\bar{\rho}_{CAZ}} + \frac{(\bar{C}_{j,CAZ} \bar{x}_{CAZ} - \bar{x}_{j,CAZ})}{\bar{\rho}_{CAZ}} \quad (12a)$$

and

$$\frac{\partial \bar{C}_{i,CAZ}}{\partial t} = \frac{\rho_r \phi}{\bar{\rho}_{CAZ} h_{CAZ}} (C_{i,r} - \bar{C}_{i,CAZ}) - \frac{\rho_\eta p}{\bar{\rho}_{CAZ} h_{CAZ}} (C_{i,\eta} - \bar{C}_{i,CAZ}) + \frac{\bar{C}_{i,CAZ} \bar{s}_{CAZ}}{\bar{\rho}_{CAZ}} + \frac{(\bar{C}_{i,CAZ} \bar{x}_{CAZ} - \bar{x}_{i,CAZ})}{\bar{\rho}_{CAZ}}. \quad (12b)$$

Eqs. (12a) and (12b) are nearly identical to Eqs. (9a) and (9b). However, colluvial transport and atmospheric deposition do not appear. Downward propagation of the weathering front is instead included, and PDZ production takes the opposite sign.

4. Sub-models

The newly developed mass balances explicitly state how each geochemical or geomorphic process contributes to the abundance of elements and minerals in a soil. In the context of our model, we review the currently available models of those processes: (1) PDZ production rate, (2) weathering front propagation rate, (3) colluvial flux, (4) chemical weathering rates of minerals, and (5) colloidal clay translocation.

4.1. The rates of PDZ production and weathering front propagation

While Ahnert (1977) made a distinction between physical soil production (equivalent to mechanical lowering of the bedrock surface in his paper) and the propagation of a chemical weathering front (equivalent to chemical lowering of the bedrock surface in his paper), it was not explicitly noted that the two processes may simultaneously occur at different depths within a single soil profile. In general, the two processes have been implicitly combined to occur at a single interface that demarcates soils and parent material; these collective processes have been termed soil or regolith production in the geomorphic literature (e.g., Humphreys and Wilkinson, 2007). Soil production rates have been long modeled as a function of the overlying soil thickness (Davis, 1892; Gilbert, 1909), and this function has been called the soil production function (e.g., Carson and Kirkby, 1972).

We use PDZ production to represent the mass flux from the CAZ (if present) or parent material to the PDZ and weathering front propagation for the mass flux from parent material to the CAZ. Several

published works, using in-situ and meteoritic cosmogenic nuclides, determined the physical production rate of the PDZ (Heimsath et al., 1997; Small et al., 1999; Heimsath et al., 2000, 2001a,b; Wilkinson et al., 2005) and chemical production rate of saprolite (Pavich, 1986, 1989), but the rates of both processes at two distinct interfaces within a single soil profile have not been considered or determined.

Two competing thoughts about the soil production function are available, and we treat the function as applicable for both PDZ production rate (p) and weathering front propagation rate (ϕ). One states that the rate exponentially decreases with increasing thickness of the overlying materials, and the other proposes that the rate peaks under a certain thickness because the overlying soil helps maintain soil moisture and presence of plants. When organisms are the major agents of PDZ production, their access to the undisturbed layer becomes increasingly difficult with increasing thickness of the PDZ. Likewise, the physical processes that break down material via freeze-thaw etc or chemical reaction between moisture and minerals may be most vigorous at an intermediate soil depth [e.g., Carson and Kirkby, 1972; Anderson, 2002]. The exponential and peak PDZ production functions and weathering front propagation rates can be described as:

$$p = p_0 e^{-\frac{h_{PDZ}}{\gamma_{PDZ}}}, \text{ or } \phi = \phi_0 e^{-\frac{h_{PDZ} + h_{CAZ}}{\gamma_{CAZ}}} \quad (13a)$$

and

$$p = \min \left[p_0 + \frac{p_p - p_0}{h_{PDZ,p}} h_{PDZ}, p_p e^{-\frac{h_{PDZ} - h_{PDZ,p}}{\gamma_{PDZ}}} \right], \quad (13b)$$

or

$$\phi = \min \left[\phi_0 + \frac{\phi_p - \phi_0}{h_{w,p}} h_w, \phi_p e^{-\frac{(h_{PDZ} + h_{CAZ}) - h_{w,p}}{\gamma_{CAZ}}} \right] \quad (13c)$$

where p_0 is the colluvial soil production rate at zero colluvial thickness [$L T^{-1}$], ϕ_0 is the weathering front propagation rate at zero soil thickness [$L T^{-1}$], p_p is the peak colluvial soil production rate [$L T^{-1}$], ϕ_p is the peak weathering front propagation rate [$L T^{-1}$], γ is a length scale describing how the colluvial soil production rate (subscript PDZ) or weathering front propagation rate (subscript CAZ) decreases with increasing depth [L], $h_{PDZ,p}$ is the colluvial thickness at the peak colluvial soil production rate [L], $h_{w,p}$ is the soil thickness at the peak weathering front propagation rate, and the function min takes the value of the minimum of the two equations within the brackets; this is one way to describe the peaked soil production function.

The depth dependency of the PDZ production or weathering front propagation is based on the assumption that the thickness of the overlying materials is the only variable determining the vertical extent of weathering agents and reagents. This approach may be reasonable for soils on eroding landscapes where the soil residence time is short. As soils age, however, soil properties other than soil thickness may further control PDZ production and weathering front propagation rates. For instance, as a soil becomes depleted in phosphorous due to mineral dissolution loss and the occlusion of the phosphorous with secondary minerals (e.g., Chadwick et al., 1999; Brenner et al., 2001), declining plant productivity may lead to the reduction of biological burrowing and of organic acidity. Likewise, the development of dense layers such as argillic horizons may dramatically affect water movement (Eppes et al., 2002), inhibiting the access of oxygen and organic acid bearing water to the deeper subsurface.

The existing functions described in Eqs. (13a) and (13b) are able to capture the rapid thickening of solum (A+B horizon) in the early phase of soil formation followed by the stabilization of solum thickness commonly seen in chronosequences (e.g., Merritts et al., 1992; White et al., 1996). It also appears that the profile development in older soils listed above tends to reduce the production rates of both

the PDZ and CAZ. Thus, while incomplete, the present functions may still be used to simulate the overall change in soil thicknesses.

4.2. PDZ flux (colluvial flux)

This paper focuses on soil bioturbation as a major process that generates colluvial flux. On level grounds ($\nabla\xi=0$, where ξ is the ground surface elevation) bioturbation moves PDZ materials in all directions with equal probability such that the net colluvial flux or the gross fluxes integrated along the entire direction becomes negligible:

$$\oint \vec{q}_{PDZ} dl = 0, \text{ where } \nabla\xi = 0. \quad (14)$$

On sloping grounds, in the upslope direction colluvial motions need to overcome both ground surface friction and gravity while flux in the downslope direction is aided by gravity (Andrews and Bucknam, 1987; Roering et al., 1999). Although soil perturbing organisms populate both level and sloping grounds, the anisotropic effects that generate net colluvial flux only occur in areas of non-zero hillslope gradient:

$$\oint \vec{q}_{PDZ} dl \neq 0 \text{ where } \nabla\xi \neq 0. \quad (15)$$

The difference between Eqs. (14) and (15) separates the soils on slopes from those on level grounds.

The colluvial flux has been described as linearly (Culling, 1963; Dietrich et al., 2003) or non-linearly (e.g., Roering et al., 1999) proportional to the slope gradient. There are indications, however, that the colluvial flux is a function of both soil thickness and slope gradient (Ahnert, 1967; Braun et al., 2001; Anderson, 2002; Furbish, 2003; Heimsath et al., 2005; Yoo et al., 2007). The linear and depth-dependant flux laws can be written respectively as:

$$\vec{Q}_{PDZ} = K \nabla\xi, \quad (16a)$$

and

$$\vec{Q}_{PDZ} = K' h_{PDZ} \nabla\xi, \quad (16b)$$

where K [$L^2 T^{-1}$] and K' [$L T^{-1}$] are constants.

Processes other than bioturbation may contribute to the colluvial flux. Rain splash and overland flow, for example, may act directly on the minerals lying on ground surface; processes acting on the surface of the soil are incorporated into the model through the variable d in the governing equations.

4.3. Mineral chemical weathering rates

Dissolution of mineral grains has often been modeled with a first order decay law, in which the rate of mass change of minerals is described as the product of a reaction coefficient (k with the unit of T^{-1}) and the mineral surface area. Conventional dissolution kinetics states that the mineral dissolution rate coefficient is a function of temperature and the chemistry of soil water (e.g., Sverdrup and Warfvinge, 1988; Lasaga 1998) and is thus independent of time. There are, however, empirical data suggesting that the reactive coefficient reduces with increasing time length that minerals are exposed to dissolution (White et al., 1996; Hodson and Langan, 1999; White and Brantley, 2003). The two competing ideas can be described by using either a constant or time-dependent mineral-specific mineral dissolution rate, k [T^{-1}]:

$$\bar{s}_{j,\tau} = -\frac{\partial m_j}{\partial \tau} = k_j \times m_j = \underbrace{(R_j \times A_j \times w_j)}_{=k_j} \times m_j, \quad (17)$$

where m_j is the mass of mineral j per volume of soil materials [$M L^{-3}$], R is chemical reaction coefficient in moles reacted per mineral surface area per time [$mol L^{-2} T^{-1}$], A is the mineral-specific surface area [$L^2 M^{-1}$], w_j is the molar weight of the considered mineral species [$M mol^{-1}$], and τ is the time length that the minerals are exposed to dissolution reaction.

Eq. (17) can be solved for the amount of remaining minerals as a function of their initial mass and the time length of dissolution exposure. In both cases the dissolution rate from the minerals declines over time because the remaining mass of minerals decreases. For the sake of simplicity in demonstrating how the rate law is incorporated into our soil model, the case of constant reactive coefficient is solved here. The mass remaining of the minerals after some elapsed time τ since the initiation of chemical weathering reaction is:

$$m_j = m_{j,0} e^{-k_j \tau}, \quad (18)$$

where $m_{j,0}$ is the mass of the mineral j in the volume of investigated soil materials at the beginning of mineral dissolution.

4.4. Clay translocation

Subsurface soil water flux also carries clay minerals. Despite being solid, the clay translocation term is included separately from colluvial flux because it follows soil water, which may have a flow direction that is distinct from the direction of colluvial flux (Table 1). Eluviation and illuviation of layered phyllosilicate clays and pedogenic iron and aluminum oxides and hydroxides have been long considered as one of the fundamental soil forming processes (Jenny and Smith, 1935). It is only recent, however, that the colloidal fluxes of clay minerals have become the subject of empirical quantification because of their role in contaminant transport (Jonge et al., 2004; McCarthy and McKay, 2004).

Clay translocation requires an independent term in our mass balance (Eqs. (9a) and (9b) to (12a) and (12b)) because its contribution to the soil's geochemical composition is distinct from those of dissolved ions in soil water and colluvial flux. Unlike chemical weathering, clay translocation contributes to the mass balance of the immobile element such as Zr (Table 1). The concentrations of elements such as Zr and Ti – generally considered insoluble – are found to be significant in clay size particles (Taboada et al., 2006). Process-based modeling of colloidal transport addressing the mobilization, translocation, and settlement of the colloidal particles is only beginning to be pursued (DeNovio et al., 2004). Initial attempts to incorporate colloidal transport into vadose zone hydrology model such as HYDRUS have been recently made (e.g., Šimunek et al., 2006), which may develop in the future to a sub-model that could be integrated into our mass balance models.

5. Implication in scaling issues

Our model offers an opportunity to systematically construct mass balances of soil systems at different spatial scales. The boundary of the modeled soil system can be defined at the scale of mineral grains to the pedon scale, and also at watershed scale (Fig. 3).

5.1. Mineral grains (laboratory) vs. pedon scales

The discrepancy between laboratory measurements of mineral dissolution rates and weathering rates measured in the field has been identified as one of the major questions in weathering science (Anderson et al., 2004). A critical task is to examine the mechanisms responsible for this discrepancy and also to correctly scale rates up from the mineral scale to the scale of a soil profile, a problem raised by Yoo and Mudd (2008). Following their approach, we consider a soil as a sum of numerous mineral grains and organic matter. The role of

t1.1 **Table 1**
Mass fluxes within and at the boundary of a soil system

Mass flux	Location	Mass phase	Agents or processes	Fractionation of minerals or elements
Surface erosion or deposition	PDZ surface	Solid	Overland flow, Aeolian deposition	Yes
PDZ production	PDZ to CAZ (or PM ^a) boundary	Solid	Biophysical perturbation	No
Weathering front propagation	CAZ-PM ^a boundary	Solid	Chemical reaction	No
Colluvial flux	PDZ	Solid	Biophysical perturbation	No
Solute flux	PDZ and CAZ	Dissolved	Soil water flux	Yes ^b
Colloidal flux	PDZ and CAZ	Solid	Soil water flux	Yes ^c

t1.10 Summary of mass fluxes described in our mass balances based on their location, phase of flux, responsible agents or processes, and their fractionating impact on soils' geochemical composition as described in our models.

t1.11 ^a Parent material.

t1.12 ^b Due to weatherability of minerals and solubility of elements.

t1.13 ^c Only suspendable fine mineral particles, which are likely to be secondary minerals, are transported.

544 organic matter can be considered by treating the elemental budget of
545 carbon. Unlike laboratory batch experiments in which minerals'
546 exposure to chemical reaction starts with the well-defined initiation
547 of the experiments, the minerals in a soil profile have the range of
548 residence times in the soil (Mudd and Furbish, 2006; Almond et al.,
549 2007; Yoo and Mudd, 2008). The PDZ, for instance, continuously
550 incorporates minerals from the underlying CAZ or fresh parent
551 material via PDZ production. Another factor determining the
552 residence time of a mineral species in the PDZ is the mineral-specific
553 susceptibility to chemical weathering. For example, plagioclase
554 minerals have less chance of surviving dissolution/leaching for a
555 given length of time than quartz.

556 Here we make two modifications to Yoo and Mudd (2008). First,
557 mineral grains are incorporated into the PDZ from the underlying CAZ,
558 the mineralogical composition of which also changes over time.
559 Second, instead of time-dependent mineral dissolution rate used in
560 Yoo and Mudd (2008), a constant rate coefficient is used for the sake
561 of simplicity. In a soil of age Γ , we first focus on a group of mineral
562 species j that entered the PDZ during the time interval between soil
563 ages of t and $t + \Delta t$. The initial mass of this mineral group is thus equal
564 to $(C_{j,CAZ,t} \rho_{CAZ} p_t) \Delta t$; the values in the parenthesis include the
565 mineralogical composition of the CAZ and the PDZ production rate.
566 The mass of this mineral group declines with soil age according to the
567 dissolution law which is a solution of Eq. (18):

569
$$m_{j,t-\Gamma} = (C_{j,CAZ,t} \rho_{CAZ} p_t) \Delta t \times e^{-k_j(\Gamma-t)}. \quad (19)$$

568 Since the soil is made up of minerals that entered the soil sometime
571 between the initiation of soil formation and Γ , the total mass of mineral

species j in the soil ($m_{j,\Gamma}$) can be represented as a sum of mineral grains
that were incorporated into the PDZ at different periods during the soil
formation and have survived dissolution and leaching:

$$m_{j,\Gamma} = \sum_{t=0}^{\Gamma} m_{j,t-\Gamma}. \quad (20)$$

575 These two equations (Eqs. (19) and (20)) allow describing the mass
576 of mineral species j that entered the PDZ at a particular period of PDZ
577 formation as a function of the soil age, PDZ production rate, and the
578 mineral-specific weathering susceptibility. Similar equations can be
579 derived for the CAZ.

582 Here we provide a heuristic application of our model. The evolution
583 of the mineralogical composition of a PDZ is simulated for the first
584 100 kyr of the soil's formation. For the sake of simplicity, PDZ is assumed
585 to develop directly from in-situ bedrock on a level geomorphic surface.
586 The process of soil production incorporates minerals from the bedrock
587 into the soil (equivalent of PDZ in this example), and the minerals
588 chemically weather in the soil. The exponential soil production function
589 is used, and this simulation focuses on soil thickness and the minerals
590 Ca-plagioclase and quartz, which are known to have dramatically
591 different chemical weathering susceptibility. For the sake of simplicity,
592 we assume that the mass loss rate of quartz mineral grains via
593 dissolution and leaching is negligible, whereas Ca-plagioclase has the
594 first order decomposition rate of 0.0001 yr^{-1} (Eq. (17)).

595 Initially the soil thickens, but the thickening rate gradually reduces
596 as the soil production rate declines (Fig. 3a). After the 100 kyr of
597 soil formation, the soil thickness reaches ~80 cm with the prescribed
598 soil production function (the parameters used fall within the range

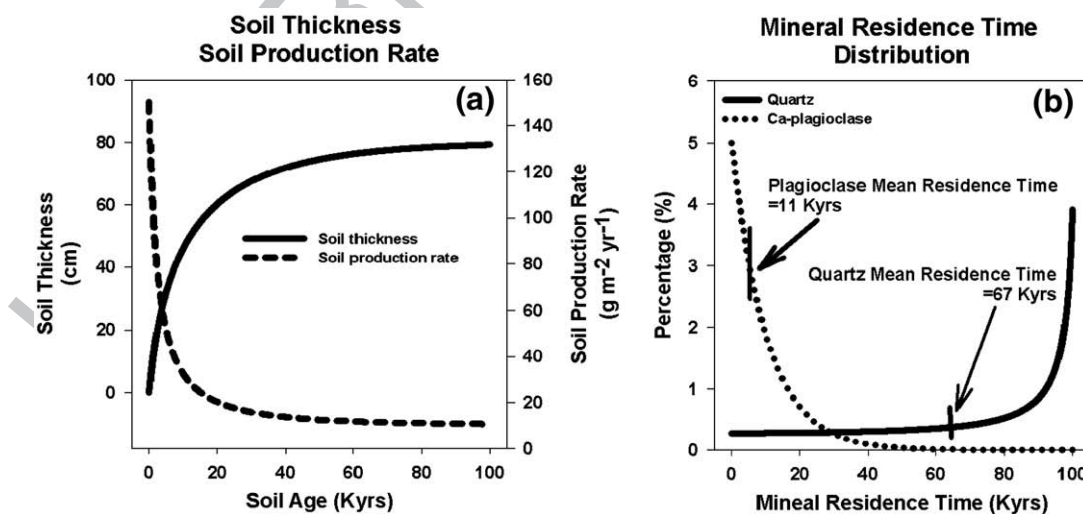


Fig. 3. Heuristic simulation of a soil formation showing the evolution of soil thickness and soil production rate (a) and the residence time distribution of the two mineral species within the simulated soil when the soil age reaches 100 kyr. Exponential soil production function (Eq. (13a)) is used with the following parameters: $p_0 = 75 \text{ m Ma}^{-1}$, $\gamma = 0.3 \text{ m}$ (Heimsath et al., 1997). Bulk densities of soil and saprolite are assumed to be 1.3 g cm^{-3} and 2.0 g cm^{-3} , respectively.

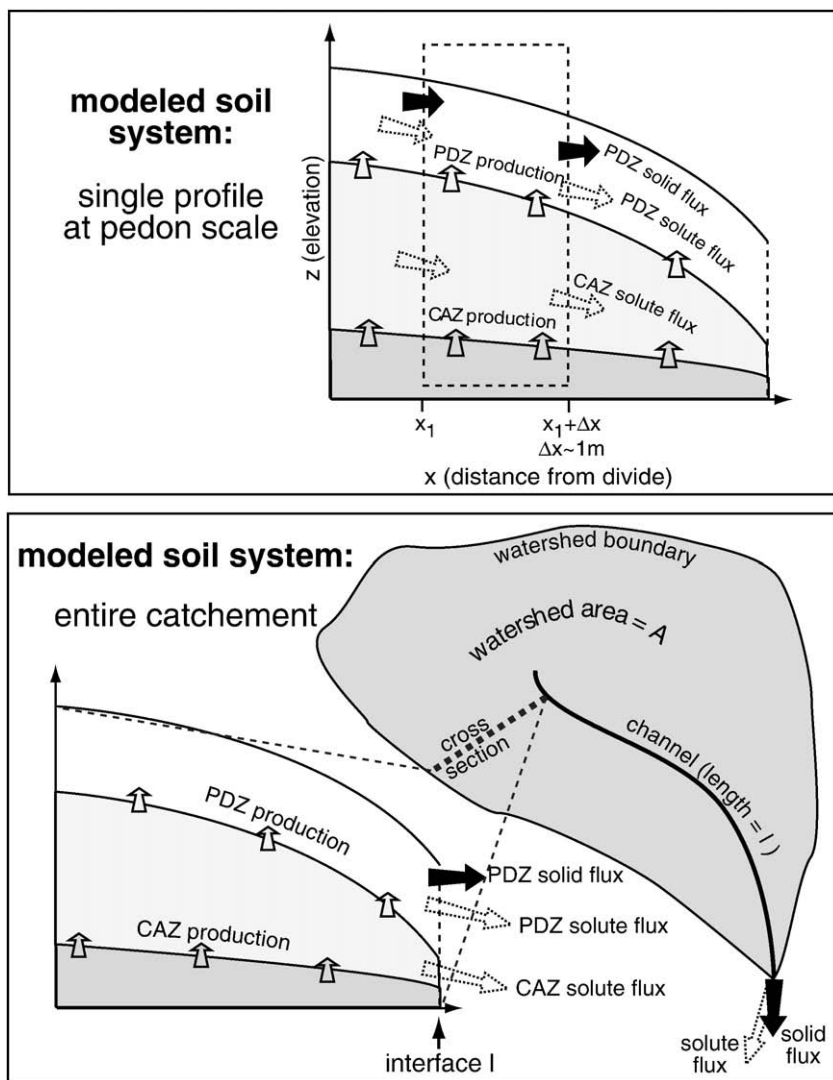


Fig. 4. Schematic showing how the model boundaries can be adjusted to address soils of different scales. In this case, we illustrate the pedon and watershed scales.

599 measured in the field, e.g., Heimsath et al., 1999). This 100 kyr old soil,
 600 however, is comprised of minerals that have dramatically different
 601 residence times in the soil. The mineral quartz, because it survives
 602 chemical weathering, continues to accumulate in the soil. Quartz
 603 grains that are introduced to the soil during the initial period of soil
 604 formation when the soil production rate is relatively high largely
 605 explain the older residence time of these minerals (Fig. 3b). In contrast,
 606 Ca-plagioclase that entered the soil in the early soil formation period
 607 has been lost from the soil. As a result, the residence time distribution
 608 of the Ca-plagioclase in the soil is skewed toward shorter residence
 609 time (Fig. 3b). This heuristic simulation shows (1) a mineral species'
 610 mean mineral residence time in a soil, regardless of its weathering
 611 susceptibility, is less than the soil age, and (2) mean residence time of
 612 a mineral species with greater susceptibility to chemical weathering
 613 will be shorter than those of weathering resistant mineral species, and
 614 (3) individual mineral grains of a same mineral species have distinct
 615 ages, and their distribution is a function of the mineral species'
 616 weathering susceptibility, soil production history, and soil age. Most
 617 importantly, this simulation shows that our model allows examining
 618 soil profiles as a sum of mineral grains and thus scaling up the
 619 laboratory based understanding of mineral grain scale chemical
 620 weathering reaction rates to soil profiles and vice versa.

621 Unlike soil age, mineral residence time can be defined and quantified
 622 for geomorphically dynamic eroding and depositional landscapes.
 623 Efforts to simulate the mineral residence time along eroding hillslope

transects have been carried out (Mudd and Furbish, 2006; Almond et al.,
 2007). In addition, by combining a detailed topographic survey with a
 colluvial transport model, Yoo et al. (2006, 2005a) estimated the time
 lengths that minerals resided in a depositional hollow since sedimenta-
 tion within a zero order watershed.

5.2. Pedon to watershed scales

The modeled soil system can be expanded to have an upper lateral
 boundary at the hillslope ridge and a lower lateral boundary at the
 basin's channels (Fig. 4). In this case the PDZ does not receive colluvial
 flux from upslope, and the outflux is simply equal to the soil erosion rate
 integrated over the watershed. Our mass balances of the PDZ (Eqs. (7a)
 and (7c)) may be recast as:

$$\frac{\partial (\bar{\rho}_{PDZ} \bar{h}_{PDZ} A)}{\partial t} = \bar{\rho}_\eta \bar{p} A + \bar{\rho}_\zeta \bar{d} A - \bar{\rho}_1 \bar{Q}_1(2l) - \bar{h}_{PDZ} \bar{s}_{PDZ} A, \quad (21a)$$

and

$$\frac{\partial (\bar{\rho}_{PDZ} \bar{C}_{i,PDZ} \bar{h}_{PDZ} A)}{\partial t} = \bar{\rho}_\eta \bar{C}_{i,\eta} \bar{p} A + \bar{\rho}_\zeta \bar{C}_{i,\zeta} \bar{d} A - \bar{\rho}_1 \bar{C}_{i,1} \bar{Q}_1(2l), \quad (21b)$$

where the overbars now represent values spatially averaged over the
 watershed, A represents the watershed area [L^2], subscript l represents
 the interface between hillslope and channel, and L represents the

642 channel length within the watershed ($2L$ is thus the length of the
643 interface between the channel and upland). Mass balances for the CAZ
644 at the watershed scale can be similarly constructed.

645 For the sake of simplicity, we assume a steady state PDZ with
646 negligible atmospheric deposition at the watershed scale, which is the
647 case considered in Riebe et al. (2004, 2003a,b, 2001):

$$649 \bar{h}_{PDZ} \bar{s}_{PDZ} = \bar{p}_n \bar{p} \left[1 - \left(\bar{C}_{i,n} / \bar{C}_{i,l} \right) \right], \quad (22)$$

648 where the underlying CAZ is also in steady state, the PDZ production
649 rate can be replaced by a weathering front propagation rate, and the
650 soil elemental chemistry at the PDZ-CAZ boundary is replaced by the
651 value of fresh parent material. In this scenario, the chemical weath-
652 ering rate is determined for the entire soil profile.

653 The result (Eq. (22)) may appear identical to the model by Riebe
654 et al. (2004, 2003a,b, 2001) (Eq. (3)), but there is an important
655 difference. In their work, catchment-averaged PDZ production rates
656 were determined by measuring cosmogenic radionuclides (such as
657 ^{10}Be and ^{26}Al) of stream sediments, which can be equated to the
658 catchment-averaged soil production rate with the steady state
659 assumption. In parallel, soil elemental chemistry was determined at
660 various positions within catchments. Our detailed derivation, how-
661 ever, reveals that the elemental chemistry of soil should be measured
662 where the soil leaves the system of interest, as noted in the subscript l
663 indicating streams. By doing so, we integrate the changes in
664 geochemical composition of PDZ due to chemical weathering during
665 the colluvial transport within the hillslope. If soil elemental composi-
666 tions vary along a hillslope transect as observed in numerous
667 hillslopes (Nezat et al., 2004; Green et al., 2006; Yoo et al., 2006),
668 correctly determining soil sampling locations for elemental or
669 mineralogical compositions is critical in determining the catchment
670 integrated chemical weathering rate as a fraction of total denudation
671 rate (see also, Mudd and Furbish, 2006).

672 To illustrate the utility of Eq. (22) in estimating the hillslope or
673 watershed integrated chemical weathering rates, we merged the
674 equation with the published toposequence data in Yoo et al. (2007)
675 (Fig. 5). Yoo et al. (2007), using the steady state form of Eq. (9a),
676 calculated pedon-scale chemical weathering rates from the ridge to the
677 hillslope base along a convex hillslope transect in Southwestern
678 Australia. For the hillslope averaged chemical weathering rate, they
679 added the pedon-scale weathering rates along the transect and then
680 divided the sum by the hillslope length. In contrast, Eq. (22) allows
681 estimating the hillslope averaged rate based on the immobile elemental
682 concentration of a pedon that is located at the hillslope base (gray circled
683 soil pedon in the Fig. 5), which makes it unnecessary to measure the

684 elemental concentrations of many soil pedons along the hillslope
685 transect. The soil at the hillslope base is the sum of minerals produced
686 and transported along the transect and thus integrates the chemical
687 weathering processes and rates within the hillslope. For the
688 hillslope transect described in Fig. 5, Yoo et al. (2007) reported the
689 hillslope averaged mass soil production rate of $47 \text{ g m}^{-2} \text{ yr}^{-1}$. By merging
690 Eq. (22) with the mass soil production rate and the Zr data in Fig. 5,
691 we have obtained the hillslope averaged chemical weathering rate of
692 $18 \text{ g m}^{-2} \text{ yr}^{-1}$, which is close to $21 \text{ g m}^{-2} \text{ yr}^{-1}$ reported by Yoo et al.
693 (2007). If the hillslope averaged Zr concentrations of both soils and
694 saprolites (values are in the Fig. 5) were used as in Riebe et al. (2004,
695 2003a,b, 2001), the hillslope averaged chemical weathering is calculated
696 to be $28 \text{ g m}^{-2} \text{ yr}^{-1}$, a value significantly higher than the estimates made
697 in this paper and in Yoo et al. (2007). This discrepancy highlights the
698 importance of correctly accounting for the boundary conditions of
699 modeled soil system across diverse spatial scales. 700

6. Implications to the emergence of soil toposequence 701

702 A soil on a hillslope transect not only receives materials from the
703 upslope but also provides materials to the soils downslope. Such series
704 of interconnected soils along a hillslope have been called soil catenas
705 (Birkeland, 1999). We do not yet have universal mathematical
706 language capable of describing how the soil catena emerges out of
707 physical and chemical processes (Yaalon, 1975). A soil catena has been
708 often considered as a product of the two interacting components
709 moving somewhat independently: skeleton (solid materials) and
710 plasma (solutes and colloidal transport via subsurface water flow)
711 (Huggett, 1975; Pedro, 1983). This concept is mathematically pre-
712 sented in our models.

713 Within the overarching theme of soil research at the landscape
714 scale (Pennock and Veldkamp, 2006), efforts to functionally relate soil
715 properties and topographic attributes such as slope gradient,
716 curvature, and distance from ridge derived from terrain analyses are
717 becoming increasingly routine (e.g., Park et al., 2001). According to our
718 model, it is the sign and magnitude of lateral physical soil fluxes
719 within the PDZ that essentially distinguish soils in different landforms
720 (Table 1). A soil's connection to its neighboring soils is profoundly
721 altered by the degree of the colluvial flux which primarily depends on
722 the slope gradient (Eq. (16a)). In the absence of slope gradient, the
723 third terms in Eqs. (9a) and (9b), which represent the geochemical
724 impact of upslope soil on the soil downslope via colluvial flux, can be
725 ignored. Thus, on level ground, a soil does not affect nor is affected by
726 neighboring soils in terms of geochemical substances (Table 2).

727 As slope gradient increases, the colluvial flux becomes a significant
728 term affecting the mass balance. Thus, a PDZ of a given volume will be
729 replaced by colluvial influx from upslope in an increasingly shorter
730 time as the slope becomes steeper (Yoo et al., 2007). Using a steady
731 state form of the PDZ mass balance, Yoo et al. (2007) calculated the
732 time length that a PDZ (defined by 1 m^2 surface area) is replaced by
733 colluvial flux from upslope along an eroding hillslope transect in a
734 semi-arid Australian landscape. The replacement time ranged
735 between 1 and 9 kyr. The replacement time can be viewed as the
736 time length that the local (hillslope position-specific) weathering
737 condition acts on the volume of the PDZ. The degree of chemical
738 weathering at a particular topographic position is the product of the
739 local chemical weathering rate and the length of time that the volume
740 of the PDZ resides at a given position.

741 A soil's distance from the hillslope ridge also contributes to
742 determining its geochemical composition because of the functional
743 relationship between minerals' weathering rate and their exposure
744 time to chemical reaction. As PDZ material moves in the downslope
745 direction, it continues to pick up mineral grains from the underlying
746 CAZ (if present) or parent material. Subsequently, mineral grains in a
747 PDZ at a certain hillslope position have a range of time lengths that
748 have elapsed since they were entrained into the PDZ. The mean

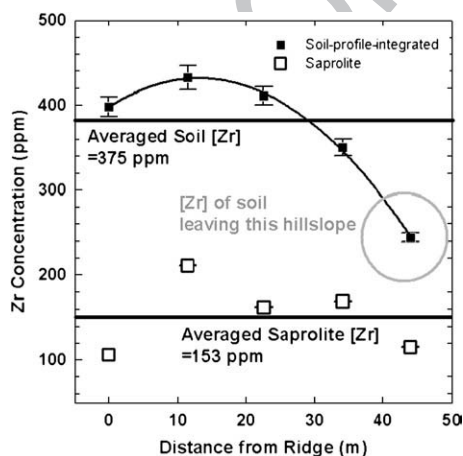


Fig. 5. Immobile Zr concentrations in the soils and saprolites along an eroding hillslope transect in Southwestern Australia (modified from Yoo et al., 2007).

Table 2
Classifying soil landforms based on the signs of gross and net colluvial fluxes and soil erosion rates

Landforms	Gross colluvial flux ^a	Colluvial flux	Soil erosion
Level landforms	$q_{ds} = q_{us}$	$\nabla Z = 0$	$\bar{Q}_{PDZ} = 0$
Flat surface			$\nabla^2 Z = 0$
Hillslope ridge			$\nabla \cdot \bar{Q}_{PDZ} = 0$
Planar slope (backslope)	$q_{ds} > q_{us}$	$\nabla Z \neq 0$	$\bar{Q}_{PDZ} > 0$
Eroding slopes (convex shoulder)	$q_{ds} > q_{us}$	$\nabla Z \neq 0$	$\bar{Q}_{PDZ} > 0$
Depositional slopes (convergent footslope and toeslope)	$q_{ds} < q_{us}$	$\nabla Z \neq 0$	$\bar{Q}_{PDZ} > 0$
			$\nabla^2 Z > 0$
			$\nabla \cdot \bar{Q}_{PDZ} > 0$
			$\nabla^2 Z = 0$
			$\nabla^2 Z > 0$
			$\nabla^2 Z < 0$
			$\nabla \cdot \bar{Q}_{PDZ} < 0$

This table is representative of landforms where colluvial flux is slope-dependent.

^a Subscripts d and u represent in downslope direction and in upslope direction, respectively.

mineral residence time in PDZ along a steadily eroding hillslope may not vary spatially, whereas transient erosion, where one portion of the hillslope is eroding at a faster rate than another, can lead to spatial variations in the mean mineral residence times (Mudd and Furbish, 2006). This can then lead to topographic variations in the degree of chemical weathering of mineral grains.

Another topographic metric that is related to soil catena is curvature. When colluvial flux is proportional to slope gradient, soil erosion, which is the difference between colluvial outflux and influx, becomes proportional to curvature. In Ruhe's and Walker (1968) slope classification system (Table 2), a shoulder is a convex (eroding) slope, while footslopes and toeslopes are convergent (depositional) slopes. Cumulative soils develop in convergent areas. Thus, curvature-dependent soil erosion or deposition controls the mass of soil per area, whereas the slope-dependent colluvial flux determines the replacement time of a volume of a PDZ. Where the PDZ production rate is a function of PDZ thickness, soil erosion (or deposition) indirectly affects the PDZ production rate by reducing (or increasing) soil thickness. Indeed, soil thickness has been found to be well correlated with local slope curvature (Heimsath et al., 1997; Heimsath et al., 2000; Yoo et al., 2006).

On level grounds the slope gradient converges to zero. Such landscapes include hillslope summits (Ruhe's and Walker, 1968). If the hillslope summit is wide enough to have negligible slope curvature, both colluvial flux and soil erosion rate become negligible, and the PDZ will thicken over time by the accumulation of materials introduced from the underlying CAZ or fresh parent material. In such cases, the mineral residence time in the PDZ becomes solely dependent of the PDZ production rate and mineral chemical weathering (Yoo and Mudd, 2008). In contrast, where the summit may be narrow and thus have a convex up topography, the parent material of the PDZ is still restricted to the underlying in-situ materials, but the residence time of the minerals within the PDZ will be determined by the sediment outflux which is in this particular case equal to soil erosion rate.

Additionally, slope curvature, by indirectly affecting PDZ production rate, may affect the variation of CAZ thickness along a soil catena. Where soil erosion rates are high, reduced soil thickness will result in conversion of CAZ material to PDZ material that is faster than the weathering front propagation. Eventually, the CAZ may thin out. This agrees with common observation that rapidly eroding soils often lack physically undisturbed B horizons or saprolite. Well developed saprolites in eroding hills, however, are also reported in Piedmont area (Pavich, 1989), indicating that the propagation of weathering front may have historically occurred at the faster rate than production of the PDZ.

Unlike the PDZ, the topographic linkage of the CAZ mass balance is not explicit. In this physically in-situ zone, the topographic impact on geochemistry, except the curvature-correlated PDZ production rate, is likely to be mediated by subsurface water flux and the pathways thereof. In our models, the interaction of water and minerals is subsumed within the chemical weathering terms which are the divergence of solute flux. The solute flux can be coupled to water chemistry through advection-dispersion-reaction models as pointed out by Mudd and Furbish (2004) and Green et al. (2006). This coupling, however, is beyond the scope of this contribution. For the

discussion of soil catenas mainly from hydrological perspective, an excellent review and synthesis is offered in Sommer and Schlichting (1997).

7. Implications for coupling soil chemical weathering and the lowering of soil-bedrock boundary

As emphasized in several preceding soil geochemistry models (Minasny and McBratney, 2001; Riebe et al., 2001, 2003a,b, 2004; Yoo et al., 2007, Yoo and Mudd, 2008), one of the appealing aspects of our mass balance is that the soil chemical weathering rate is functionally coupled to physical and chemical processes that lower the elevation of the soil-bedrock boundary. For the sake of simplicity, we assume here that translocation and atmospheric deposition are negligible:

$$S_{PDZ} = \rho_n p \left(1 - \frac{C_{i,n}}{\bar{C}_{i,PDZ}} \right) + \frac{\nabla \bar{C}_{i,PDZ}}{\bar{C}_{i,PDZ}} \bar{\rho}_{PDZ} \bar{Q}_{PDZ} + \frac{\bar{\rho}_{PDZ} h_{PDZ}}{\bar{C}_{i,PDZ}} \frac{\partial \bar{C}_{i,PDZ}}{\partial t} \quad (23)$$

The first term in Eq. (23) describes how the PDZ is enriched in immobile soil components relative to the underlying CAZ. Thus, the chemical weathering rate and PDZ production rate are positively related in PDZ. The same logic applies to the colluvial flux. If the PDZ becomes enriched in the immobile soil component in the direction of colluvial flux (that is, the downslope direction on hillslopes), the positive proportionality holds between the chemical weathering rate and colluvial flux. These two terms therefore demonstrate how the chemical weathering rate in the PDZ is limited by mineral supply via the two physical processes. A steady state mass balance of the PDZ (Eq. (23) time derivatives set to zero) has been applied to field data (Yoo et al., 2007); this work showed that the chemical weathering term associated with colluvial flux (the 2nd term in Eq. (23)) dominated the total chemical weathering rate on a convex hillslope in a semi-arid landscape in Southwestern Australia.

In the CAZ where physical disturbance is absent, the interaction between physical and chemical weathering processes is expected to be more subtle. As done in Eq. (23), the CAZ chemical weathering rate can be formulated as a function of PDZ production rate. For the sake of simplicity, we assume here that translocation is negligible:

$$S_{CAZ} = -\rho_n p \left(1 - \frac{C_{i,n}}{\bar{C}_{i,CAZ}} \right) + \rho_r \phi \left(1 - \frac{C_{i,r}}{\bar{C}_{i,CAZ}} \right) + \frac{\bar{\rho}_{CAZ} h_{CAZ}}{\bar{C}_{i,CAZ}} \frac{\partial \bar{C}_{i,CAZ}}{\partial t} \quad (24)$$

Interpretation of this model can be facilitated by discussing a special steady state case (the time derivative in Eq. (24) is zero) in which the immobile elemental concentration of CAZ is constant. Eq. (24) is then simplified to

$$S_{CAZ} = p \left[\left(\rho_r - \rho_n \right) + \frac{1}{\bar{C}_{i,CAZ}} \underbrace{\left(\rho_n C_{i,n} - \rho_r C_{i,r} \right)}_{= 0 \text{ in isovolumetric weathering}} \right] \quad (25)$$

The second term in the bracket becomes zero if the CAZ is saprolite that has experienced isovolumetric weathering. In such cases, the

847 profile weighted chemical weathering rate from the saprolite is simply
848 the product of the PDZ production rate (which is equivalent to the
849 weathering front propagation rate) and the bulk density difference
850 between the fresh parent material and the material entering the PDZ
851 from the CAZ.

852 The depth integrated chemical weathering rate for the entire soil
853 thickness (PDZ+CAZ), when the soil is in steady state and the CAZ is
854 isovolumetrically weathered saprolite, can be written as:

$$856 S_{\text{total}} = S_{\text{PDZ}} + S_{\text{CAZ}} = p \left[\rho_{\eta} C_{i,\eta} \left(\underbrace{\frac{1}{C_{i,\text{CAZ}}} - \frac{1}{C_{i,\text{PDZ}}}}_{>0} \right) + \underbrace{(\rho_{\tau} - \rho_{\eta})}_{>0} \right]. \quad (26)$$

855 The quantities in the parentheses are likely to be positive. The
856 concentration of a weathering resistant soil component is likely to be
857 greater in the PDZ than in the CAZ. Likewise, the bulk density at the
858 PDZ and CAZ boundary is likely to be less than that of fresh parent
859 materials. Thus, the model suggests that the total soil chemical
860 weathering rate is positively related to the rates of PDZ production (p)
861 and weathering front propagation ($\phi = p$ at steady state).

864 8. Conclusions

865 We have combined widely used models of hillslope sediment
866 transport and geochemical mass balance to explicitly address the
867 geochemical evolution of soils across diverse landscapes. The model,
868 capable of integrating recent advances in geochemistry and geomor-
869 phology, can be fully parameterized with empirical data generated in
870 field and laboratory settings. Furthermore, the model provides a
871 framework to integrate the findings from theoretical, laboratory, and
872 field based studies. The key message of the model is that chemical
873 reactions of minerals occur during the movement of the minerals via
874 various physical processes at different scales.

875 The models presented in this paper may be used in offering a
876 phenomenological and mechanistic basis for explaining the statistical
877 relationships among topographic attributes and various soil geochemical
878 properties which are becoming increasingly available with the advances
879 of digital mapping tools (Pennock and Veldkamp 2006). Furthermore,
880 the models can be integrated with carbon cycling to better understand
881 the dynamics of soil carbon storage at landscape scales. Spurred by the
882 interests in the net carbon exchange between soils and the atmosphere
883 (e.g., Stallard, 1998), the impact of hillslope sediment flux on soil carbon
884 budgets has begun to be investigated (Rosenbloom et al., 2001; Yoo et al.,
885 2005a, 2006). The ultimate goal we want to achieve with this model in
886 the future is to quantitatively reproduce the observed temporal and
887 spatial variation of soils' geochemical profiles by combining our models
888 with a suite of well-defined physical and chemical processes independ-
889 ently measured in field and laboratory settings.

Q4890 9. Uncited reference

891 Soil-Science-Society-of-America, 2001

892 Acknowledgements

893 We thank three anonymous reviewers for their thoughtful and
894 detailed comments.

895 Appendix A. List of symbols

896 Variables and parameters

898	A	mineral-specific surface area [$L^2 M^{-1}$]
899	C	mass concentration [$M M^{-1}$]
900	d	deposition or erosion rate at ground surface [$L T^{-1}$]
901	h	thickness [L]

	k	mineral dissolution rate [T^{-1}]	902
	K	constant in slope-dependent sediment flux [$L^3 L^{-1} T^{-1}$]	903
	K'	constant in slope product soil thickness dependent sediment flux [$L^2 L^{-1} T^{-1}$]	904 905
	l	channel length within a watershed [L]	906
	m	mass of a mineral species per volume of soil materials [$M L^{-3}$]	907
	p	PDZ production rate [$L T^{-1}$]	908
	q	volume of gross sediment flux crossing unit contour line [$L^3 L^{-1} T^{-1}$]	909 910
	Q	volume of sediment flux crossing unit contour line [$L^3 L^{-1} T^{-1}$]	911
	R	chemical reaction coefficient in moles reacted per mineral surface area per time [$mol L^{-2} T^{-1}$]	912 913
	s	rate that soil mass is lost/gained via chemical weathering per unit soil volume [$M L^{-3} T^{-1}$]	914 915
	S	mass loss rate by chemical weathering [$M L^{-2} T^{-1}$]	916
	t	time [T]	917
	x	rate that soil mass is lost/gained due to clay translocation per unit soil volume [$M L^{-3} T^{-1}$]	918 919
	w	molar weight of a mineral species [$M mol^{-1}$]	920
	δ	mass loss during soil formation [$M L^{-2}$]	921
	ϕ	weathering front propagation rate [$L T^{-1}$]	922
	γ	length scale describing the depth dependency of PDZ and CAZ production rates [L^{-1}]	923 924
	η	elevation of PDZ to CAZ boundary [L]	925
	μ	elevation of the boundary between CAZ and fresh parent material	926 927
	ρ	bulk density [$M L^{-3}$]	928
	τ	time length that minerals are exposed to dissolution reaction [T]	929 930
	ξ	elevation of ground surface [L]	931

Subscripts

	i	immobile soil component	933
	l	interface between hillslope and channel	935
	o	value when soil thickness is zero	936 937
	p	peak value	938
	r	fresh parent material	939
	w	soil	940

References

- Ahnert, F., 1967. The role of equilibrium concept in the interpretation of landforms of
fluvial erosion and deposition. In: Macar, P. (Ed.), L'evolution des Versants. 943
University of Liege, Liege, France, pp. 23-41. 945
- Ahnert, F., 1977. Some comments on the quantitative formulation of geomorpho- 946
logical processes in a theoretical model. Earth Surface Processes and Landforms 2, 947
191-201. 948
- Almond, P., Hales, T.C., Roering, J.J., 2007. Using soil residence time to delineate spatial 949
and temporal patterns of landscape disequilibrium. Journal of Geophysical 950
Research-Earth Surface 112 (F3), F03S17. doi:10.1029/2006JF000568. 951
- Amundson, R., 2004. In: Holland, H.D., Turekian, K.K. (Eds.), Soil Formation. Treatise on 952
Geochemistry, vol. 5. Elsevier Science Ltd., Oxford, UK, pp. 1-35. 953
- Anderson, R.S., 2002. Modeling the tor-dotted crests, bedrock edges, and parabolic 954
profiles of high alpine surfaces of the Wind River Range, Wyoming. Geomorphology 955
46 (1-2), 35-58. 956
- Anderson, S.P., Blum, J., Brantley, S.L., Chadwick, O., Chorover, J., Derry, L.A., Drever, J.L., 957
Hering, J.G., Kirchner, J.W., Kump, L.R., Richter, D., White, A.F., 2004. Proposed 958
initiative would study earth's weathering engine. EOS 85, 265-269. 959
- Andrews, D.J., Bucknam, R.C., 1987. Fitting degradation of shoreline scarps by a 960
nonlinear diffusion model. Journal of Geophysical Research 92, 12857-12867. 961
- April, R., Newton, R., Coles, L.T., 1986. Chemical-weathering in 2 Adirondack watersheds - 962
past and present-day rates. Geological Society of America Bulletin 97 (10), 1232-1238. 963
- Becker, G.F., 1895. Reconnaissance of the gold fields of the southern Appalachians. In: 964
Interior, D.o. (Ed.), Volume Sixteenth annual report of the United States Geological 965
Survey to the Secretary of the Interior 1894-1895, Part III - Mineral resources of 966
the United States, 1894 metallic products. U.S. Gov. Print Office, Washington, DC., 967
pp. 252-331. 968
- Bierman, P.R., Nichols, K.K., 2004. Rock to sediment-slope to sea with ^{10}Be -rates of 969
landscape change. Annual Review of Earth and Planetary Sciences 32, 215-255. 970
- Birkeland, P.W., 1999. Soils and Geomorphology. Oxford University Press, New York. 430 p. 971
- Birkeland, P.W., Berry, M.E., 1991. Use of soil catena field data for estimating relative ages 972
of moraines. Geology 19, 281-283. 973
- Braun, J., Heimsath, A.M., Chappell, J., 2001. Sediment transport mechanisms on soil- 974
mantled hillslopes. Geology 29, 683-686. 975

- Brenner, D.L., Amundson, R., Baisden, W.T., et al., 2001. Soil N and N₂-15 variation with time in a California annual grassland ecosystem. *Geochimica et Cosmochimica Acta* 65 (22), 4171–4186.
- Brimhall, G.H., Dietrich, W.E., 1987. Constitutive mass balance relations between chemical composition, volume, density, porosity, and strain in metasomatic hydrochemical systems: results on weathering and pedogenesis. *Geochimica et Cosmochimica Acta* 51, 567–587.
- Brimhall, G.H., Lewis, C.J., Ague, J.J., Dietrich, W.E., Hampel, J., Teague, T., Rix, P., 1988. Metal enrichment in bauxites by deposition of chemically mature aeolian dust. *Nature* 333, 819–824.
- Buol, S.W., Southard, R.J., Graham, R.C., McDaniel, P.A., 1997. *Soil Genesis and Classification*. Iowa State Press, Ames, Iowa. 494 p.
- Carson, M.A., Kirkby, M.J., 1972. *Hillslope Form and Process*. Cambridge University Press, Cambridge. 475 p.
- Chadwick, O.A., Derry, L.A., Vitousek, P.M., Huebert, B.J., Hedin, L.O., 1999. Changing sources of nutrients during four million years of ecosystem development. *Nature* 397, 491–497.
- Culling, W.E.H., 1963. Soil creep and the development of hillside slopes. *The Journal of Geology* 71, 127–161.
- Davis, W.M., 1892. The Convex profile of badland divides. *Science* 20, 245.
- DeNovio, N.M., Saiers, J.E., Ryan, J.N., 2004. Colloid movement in unsaturated porous media: recent advances and future directions. *Vadose Zone Journal* 3, 338–351.
- Dietrich, W.E., Reiss, R., Hsu, M.L., Montgomery, D.R., 1995. A process-based model for colluvial soil depth and shallow landsliding using digital elevation data. *Hydrological Processes* 9, 383–400.
- Dietrich, W.E., Bellugi, D.G., Sklar, L.S., Stock, J.D., Heimsath, A.M., Roering, J.J., 2003. Geomorphic transport laws for predicting landscape form and dynamics. In: Wilcock, P.R., Iverson, R.M. (Eds.), *Predictions in Geomorphology*. Geophysical Monograph Series, vol. 135. American Geophysical Union, Washington D.C., pp. 103–132.
- Eppes, M.C., McFadden, L.D., Matti, J., Powell, R., 2002. Influence of soil development on the geomorphic evolution of landscapes: an example from Transverse Ranges of California. *Geology* 30, 195–198.
- Furbish, D.J., 2003. Using the dynamically coupled behavior of land surface geometry and soil thickness in developing and testing hillslope evolution models. In: Wilcock, P.R., Iverson, R.M. (Eds.), *Predictions in geomorphology*. Geophysical Monograph Series, vol. 135. American Geophysical Union, Washington D.C., pp. 169–181.
- Gabet, E., Reichman, O., Seabloom, E., 2003. The effects of bioturbation on soil processes and sediment transport. *Annual Review of Earth and Planetary Sciences* 31, 249–273.
- Gilbert, G.K., 1909. The convexity of hilltops. *Journal of Geology* 17, 344–350.
- Green, E.G., Dietrich, W.E., Banfield, J.F., 2006. Quantification of chemical weathering rates across an actively eroding hillslope. *Earth and Planetary Science Letters* 242, 159–169.
- Heimsath, A.M., Dietrich, W.E., Nishiizumi, K., Finkel, R.C., 1997. The soil production function and landscape equilibrium. *Nature* 388, 358–361.
- Heimsath, A.M., Dietrich, W.E., Nishiizumi, K., Finkel, R.C., 1999. Cosmogenic nuclides, topography, and the spatial variation of soil depth. *Geomorphology* 27, 151–172.
- Heimsath, A.M., Chappell, J., Dietrich, W.E., Nishiizumi, K., Finkel, R.C., 2000. Soil production on a retreating escarpment in southeastern Australia. *Geology* 28, 787–790.
- Heimsath, A.M., Chappell, J., Dietrich, W.E., Nishiizumi, K., Finkel, R.C., 2001a. Late Quaternary erosion in southeastern Australia: a field example using cosmogenic nuclides. *Quaternary International* 83–85, 169–185.
- Heimsath, A.M., Chappell, J., Dietrich, W.E., Nishiizumi, K., Finkel, R.C., 2001b. Stochastic processes of soil production and transport: erosion rates, topographic variation, and cosmogenic nuclides in the Oregon Coast Range. *Earth Surface Processes and Landforms* 26, 531–552.
- Heimsath, A.M., Furbish, D.J., Dietrich, W.E., 2005. The illusion of diffusion: field evidence for depth dependent sediment transport. *Geology* 33, 949–952.
- Hodson, M.E., Langan, S.J., 1999. The influence of soil age on calculated mineral weathering rates. *Applied Geochemistry* 14 (3), 387–394.
- Hole, F.D., 1961. A classification of pedoturbation and some other processes and factors of soil formation in relation to isotropism and anisotropism. *Soil Science* 91, 375–377.
- Hole, F.D., 1981. Effects of animals on soil. *Geoderma* 25, 75–112.
- Huggett, R., 1975. Soil and landscape systems — a model of soil genesis. *Geoderma* 13, 1–22.
- Humphreys, G.S., Wilkinson, M.T., 2007. The soil production function: a brief history and its rediscovery. *Geoderma* 139 (1–2), 73–78.
- Jenny, H., 1941. *The Factors of Soil Formation*. McGraw-Hill, New York. 281 p.
- Jenny, H., Smith, G.D., 1935. Colloid transport aspects of clay pan formation in soil profiles. *Soil Science* 39, 377–379.
- Johnson, D.L., 1990. Biomantle evolution and the redistribution of earth materials and artifacts. *Soil Science* 149, 84–102.
- Johnson, D.L., 1994. Reassessment of early and modern soil horizon designation frameworks and associated pedogenic processes: are midlatitude A E B₁–C horizons equivalent to tropical M S W horizons? *Soil Science (Trends in Agricultural Science)* 77–91.
- Jonge, L.W.d., Kjaergaard, C., Moldrup, P., 2004. Colloids and colloid-facilitated transport of contaminants in soils: an introduction. *Vadose Zone Journal* 3, 321–325.
- Kirkby, M.J., 1977. Soil development models as a component of slope models. *Earth Surface Processes and Landforms* 2 (2–3), 203–230.
- Kirkby, M.J., 1985. A basis for soil-profile modeling in a geomorphic context. *Journal of Soil Science* 36 (1), 97–121.
- Kurtz, A.C., Derry, L.A., Chadwick, O.A., Alfano, M.J., 2000. Refractory element mobility in volcanic soils. *Geology* 28, 683–686.
- Lasaga, A.C., 1998. *Kinetic Theory in the Earth Sciences*. Princeton Series in Geochemistry. Princeton University Press, Princeton, N.J. 811 pp.
- Marshall, C.E., Haseman, J.F., 1942. The quantitative evaluation of soil formation and development by heavy mineral studies: a Grundy silt loam study. *Soil Science Society of America Proceedings* 7, 448–453.
- McCarthy, J.F., McKay, L.D., 2004. Colloid transport in the subsurface: past, present, and future challenges. *Vadose zone Journal* 3, 326–327.
- McKean, J.A., Dietrich, W.E., Finkel, R.C., Southon, J.R., Caffee, M.W., 1993. Quantification of soil production and downslope creep rates from cosmogenic ¹⁰Be accumulations on a hillslope profile. *Geology* 21, 343–346.
- Merritts, D.J., Chadwick, O.A., Hendricks, D.M., Brimhall, G.H., Lewis, C.J., 1992. The mass balance of soil evolution on late Quaternary marine terraces, northern California. *Geological Society of America Bulletin* 104, 1456–1470.
- Minasny, B., McBratney, A.B., 1999. A rudimentary mechanistic model for soil production and landscape development. *Geoderma* 90, 3021.
- Minasny, B., McBratney, A.B., 2001. A rudimentary mechanistic model for soil formation and landscape development II. A two-dimensional model incorporating chemical weathering. *Geoderma* 103, 161–179.
- Minasny, B., McBratney, A.B., 2006. Mechanistic soil-landscape modelling as an approach to developing pedogenetic classifications. *Geoderma* 133, 138–149.
- Monaghan, M.C., McKean, J., Dietrich, W., Klein, J., 1992. ¹⁰Be chronometry of bedrock-to-soil conversion rates. *Earth and Planetary Science Letters* 111, 483–492.
- Mudd, S.M., Furbish, D.J., 2004. Influence of chemical denudation on hillslope morphology. *Journal of Geophysical Research—Earth Surface* 109, F02001. doi:10.1029/2003JF000087.
- Mudd, S.M., Furbish, D., 2006. On the use of chemical tracers to constrain mechanical and chemical denudation processes on hillslopes. *Journal of Geophysical Research—Earth Surface* 111 (F2), F02021. doi:10.1029/2005JF00343.
- Mudd, S.M., Furbish, D.J., 2007. Responses of soil-mantled hillslopes to transient channel incision rates. *Journal of Geophysical Research—Earth Surface* 112 (F3), F03S18. doi:10.1029/2006JF000516.
- Munsell Color, 2000. *Munsell Soil Color Chart*. Baltimore, Md., 22 p.
- Nezat, C.A., Blum, J.D., Klauze, A., Johnson, C.E., Siccama, T.G., 2004. Influence of landscape positions and vegetation on long-term weathering rates at the Hubbard Brook Experimental Forest, New Hampshire, USA. *Geochimica et Cosmochimica Acta* 68, 3065–3078.
- Park, S.J., McSweeney, K., Lowery, B., 2001. Identification of the spatial distribution of soils using a process-based terrain characterization. *Geoderma* 103, 249–272.
- Pavich, M.J., 1986. Ch. 23 processes and rates of saprolite production and erosion on a foliated granitic rock of the Virginia Piedmont. In: Colman, S.M., Dethier, D.P. (Eds.), *Rates of Chemical Weathering of Rocks and Minerals*. Academic Press, Orlando, Florida, pp. 551–590.
- Pavich, M.J., 1989. Regolith residence time and the concept of surface age of the Piedmont “Peneplain”. *Geomorphology* 2, 181–196.
- Pedro, G., 1983. Structuring of some basic pedological processes. *Geoderma* 31, 289–299.
- Pennock, D.J., Veldkamp, A., 2006. Advances in landscape-scale soil research. *Geoderma* 133, 1–5.
- Rasmussen, C., Tabor, N.J., 2007. Applying a quantitative pedogenic energy model across a range of environmental gradients. *Soil Science Society of America Journal* 71 (6), 1719–1729.
- Riebe, C.S., Kirchner, J.W., Granger, D.E., Finkel, R.C., 2001. Minimal climatic control on erosion rates in the Sierra Nevada, California. *Geology* 29, 447–450.
- Riebe, C.S., Kirchner, J.W., Finkel, R.C., 2003a. Long-term rates of chemical weathering and physical erosion from cosmogenic nuclides and geochemical mass balance. *Geochimica et Cosmochimica Acta* 67, 4411–4427.
- Riebe, C.S., Kirchner, J.W., Finkel, R.C., 2003b. Sharp decrease in long-term chemical weathering rates along an altitudinal transect. *Earth and Planetary Science Letters* 218, 421–434.
- Riebe, C.S., Kirchner, J.W., Finkel, R.C., 2004. Erosional and climatic effects on long-term chemical weathering rates in granitic landscapes spanning diverse climate regimes. *Earth and Planetary Science Letters*.
- Roering, J.J., Gerber, M., 2005. Fire and the evolution of steep, soil-mantled landscapes. *Geology* 33 (5), 349–352.
- Roering, J.J., Kirchner, J.W., Dietrich, W.E., 1999. Evidence for nonlinear, diffusive sediment transport on hillslopes and implications for landscape morphology. *Water Resources Research* 35, 853–870.
- Roering, J.J., Kirchner, J.W., Dietrich, W.E., 2001. Hillslope evolution by nonlinear, slope-dependent transport: steady state morphology and equilibrium adjustment timescales. *Journal of Geophysical Research—Solid Earth* 106 (B8), 16499–16513.
- Roering, J.J., Almond, P., Tonkin, P., McKean, J., 2004. Constraining climatic controls on hillslope dynamics using a coupled model for the transport of soil and tracers: application to loess-mantled hillslopes, South Island, New Zealand. *Journal of Geophysical Research—Earth Surface* 109, F01010. doi:10.1029/2003JF000034.
- Rosenbloom, N.A., Doney, S.C., Schimel, D.S., 2001. Geomorphic evolution of soil texture and organic matter in eroding landscapes. *Global Biogeochemical Cycles* 15, 1133–1134.
- Ruhe, R.V., Walker, P.H., 1968. Hillslope models and soil formation. I. Open systems. *Transactions of the 9th International Congress on Soil Science* 6 (4), 551–560.
- Salvador-Blanes, S., Minasny, B., McBratney, A.B., 2007. Modelling long-term *in situ* soil profile evolution: application to the genesis of soil profiles containing stone layers. *European Journal of Soil Science* 58, 1535–1548.
- Schaetzl, R., Anderson, S., 2005. *Soil: Genesis and Geomorphology*. Cambridge, 817 p.
- Simonson, R.W., 1959. Outline of a generalized theory of soil genesis. *Soil Science Society of America Proceedings* 23, 152–156.
- Šimunek, J., He, C., Pang, J.L., Bradford, S.A., 2006. Colloid-facilitated transport in variably-saturated porous media: numerical model and experimental verification. *Vadose Zone Journal* 5, 1035–1047.
- Small, E.E., Anderson, R.S., Hancock, G.S., 1999. Estimates of the rate of regolith production using ¹⁰Be and ²⁶Al from an alpine hillslope. *Geomorphology* 27, 131–150.

- 1148 Soil Science Society of America, 2001. Glossary of Soil Science Terms. Soil Science
1149 Society of America. 140 p.
- 1150 Soil Survey Division Staff, 1993. Soil survey manual. Soil Conservation Service. U.S.
1151 Department of Agriculture Handbook 18.
- 1152 Sommer, M., Schlichting, E., 1997. Archetypes of catenas in respect to matter—a concept
1153 for structuring and grouping catenas. *Geoderma* 76, 1–33.
- 1154 Stallard, R.F., 1998. Terrestrial sedimentation and the carbon cycle: coupling weathering
1155 and erosion to carbon burial. *Global Biogeochemical Cycles* 12 (2), 231–257.
- 1156 Sverdrup, H., Warfvinge, P., 1988. Weathering of primary silicate minerals in the natural
1157 soil environment in relation to a chemical weathering model. *Water Air and Soil
1158 Pollution* 38 (3–4), 387–408.
- 1159 Taboada, T., Cortizas, A.M., García, C., García-Rodeja, E., 2006. Particle-size fractionation
1160 of titanium and zirconium during weathering and pedogenesis of granitic rocks in
1161 NW Spain. *Geoderma* 131, 218–236.
- 1162 Tandarich, J.P., Darmody, R.G., Follmer, L.R., Johnson, D.L., 2002. Historical development
1163 of soil and weathering profile concepts from Europe to the United States of America.
1164 *Soil Science Society of America* 66, 335–343.
- 1165 White, A., Brantley, S., 2003. The effect of time on the weathering of silicate minerals:
1166 why do weathering rates differ in the laboratory and field? *Chemical Geology* 202,
1167 479–506.
- 1168 White, A.F., Blum, A.E., Schulz, M.S., Bullen, T.D., Harden, J.W., Peterson, M.L., 1996. Chemical
1169 weathering rates of a soil chronosequence on granitic alluvium: 1. Quantification of
1170 mineralogical and surface area changes and calculation of primary silicate reaction
1171 rates. *Geochimica et Cosmochimica Acta* 60, 2533–2550.
- Wilkinson, M.T., Chappell, J., Humphries, G.S., Fitfield, K., Smith, B., Hesse, P., 2005. Soil
1172 production in heath and forest, Blue Mountains, Australia: influence of lithology
1173 and palaeoclimate. *Earth Surface Processes and Landforms* 30 (8), 923–934. 1174
- Yaalon, D.H., 1975. Conceptual models in pedogenesis: can soil-forming functions be solved?
1175 *Geoderma* 14, 189–205. 1176
- Yoo, K., Mudd, S.M., 2008. The discrepancy between mineral residence time and soil age:
1177 implications for the interpretation of chemical weathering rates. *Geology* 36 (1),
1178 0.35–0.38. doi:10.1130/G24285A. 1179
- Yoo, K., Amundson, R., Heimsath, A.M., Dietrich, W.E., 2005a. Erosion of upland hillslope
1180 soil organic carbon: coupling field measurements with a sediment transport model.
1181 *Global Biogeochemical Cycles* 19 Art. No. GB3003. 1182
- Yoo, K., Amundson, R., Heimsath, A.M., Dietrich, W.E., 2005b. A process based model
1183 linking pocket gopher (*Thomomys bottae*) activity to sediment transport and soil
1184 thickness. *Geology* 33, 917–920. 1185
- Yoo, K., Amundson, R., Heimsath, A.M., Dietrich, W.E., 2006. Spatial patterns of soil
1186 organic carbon on hillslopes: integrating geomorphic processes and the biological C
1187 cycle. *Geoderma* 130, 47–65. 1188
- Yoo, K., Amundson, R., Heimsath, A.M., Dietrich, W.E., Brimhall, G., 2007. Integration of
1189 geochemical mass balance with sediment transport to calculate rates of soil chemical
1190 weathering and transport on hillslopes. *Journal of Geophysical Research* 112, F02013. 1191
doi:10.1029/2005JF000402. 1192
1193